*Manuscript
Click here to download Manuscript: REVISED-PARP-Tumors-Main-Manuscript 20-11-2015.docx Click here to view linked References

REDUCED TUMOR BURDEN THROUGH INCREASED OXIDATIVE STRESS IN LUNG ADENOCARCINOMA CELLS OF PARP-1 AND PARP-2 KNOCKOUT MICE

Mercè Mateu-Jiménez[1,2], Blanca Cucarull-Martínez[1], Jose Yelamos[3,4] and Esther Barreiro[1,2]

[1]Pulmonology Department-Lung Cancer Research group, IMIM-*Hospital del Mar*, Health and Experimental Sciences Department (CEXS), *Universitat Pompeu Fabra* (UPF), Barcelona Biomedical Research Park (PRBB), C/ Dr. Aiguader, 88, Barcelona.

[2]*Centro de Investigación en Red de Enfermedades Respiratorias* (CIBERES), *Instituto de Salud Carlos* III (ISCIII), Barcelona, Spain.

[3]Cancer Research Program, Hospital del Mar Medical Research Institute (IMIM), Barcelona, Spain

[4]*Centro de Investigación en Red de Enfermedades Hepáticas y Digestivas* (CIBERehd), *Instituto de Salud Carlos* III (ISCIII), Barcelona, Spain.

Corresponding author: Dr. Esther Barreiro, Lung Cancer Research Group, IMIM-Hospital del Mar, PRBB, C/ Dr. Aiguader, 88, Barcelona, E-08003 Spain, Telephone: (+34) 93 316 0385, Fax: (+34) 93 316 0410, e-mail: ebarreiro@imim.es.

Short title: Biochemical mechanisms in tumor progression of mice deficient in PARP-1 and -2

Word count: 3,384

ABSTRACT

Lung cancer (LC) is currently a major leading cause of cancer deaths worldwide. Poly(ADP-ribose) polymerases (PARP)-1 and -2 play important roles in DNA repair and other cell functions. Oxidative stress triggers autophagy and apoptosis. PARP inhibitors are currently used as anticancer strategies including LC. We hypothesized that inhibition of either PARP-1 or -2 expressions in the host animals influences tumor burden through several biological mechanisms, mainly redox imbalance (enhanced oxidative stress and/or decreased antioxidants, and cell regulators) in wild type (WT) lung adenocarcinoma cells. Compared to WT control tumors, in those of Parp-$1^{-/-}$ and Parp-$2^{-/-}$ mice: 1) tumor burden, as measured by weight, and cell proliferation rates were decreased, 2) oxidative stress levels were greater, whereas those of the major antioxidant enzymes were lower especially catalase, 3) tumor apoptosis and autophagy levels were significantly increased, and 4) miR-223 and nuclear factor of activated T-cells (NFAT)c-2 expression was decreased (the latter only in Parp-$1^{-/-}$ mice). Furthermore, whole body weight gain at the end of the study period also improved in Parp-$1^{-/-}$ and Parp-$2^{-/-}$ mice compared to WT animals. We conclude that PARP-1 and -2 genetic deletions in the host mice induced a significant reduction in tumor burden most likely through alterations in redox balance (downregulation of antioxidants, NFATc-2 and miR223, and increased oxidative stress), which in turn led to increased apoptosis and autophagy. Furthermore, tumor progression was also reduced probably as a result of cell cycle arrest induced by PARP-1 and -2 inhibition in the host mice. These results highlight the relevance of the host status in tumor biology, at least in this experimental model of lung adenocarcinoma in mice. Future research will shed light on the effects of selective pharmacological inhibitors of PARP-1 and PARP-1 in the host and tumor burden, which could eventually be applied in actual clinical settings. **Word count**: 300

KEY WORDS: lung adenocarcinoma tumors; Parp-$1^{-/-}$ and Parp-$2^{-/-}$ mice; redox imbalance; autophagy; apoptosis; tumor proliferation.

1. INTRODUCTION

Lung cancer (LC) is the most prevalent cancer nowadays. Moreover, it is the leading cause of cancer deaths worldwide, with an overall survival rate lower than 15% in five years [1,2]. Cigarette smoke and other noxious particles that promote lung carcinogenesis are probably the main etiologic factors of LC [3,4]. Despite that the study of LC has received much attention in the last years, the lack of appropriate methodologies for the early diagnosis together with the absence of safe targeted therapies, are probably the main reasons accounting for its poor prognosis [5-10].

Poly(ADP-ribosyl)ation is a posttranscriptional modification by which poly(ADP-ribose) polymerases (PARPs) polymerize poly(ADP-ribose) on acceptor proteins using NAD^+ as a substrate [11]. PARP-1 and PARP-2 are the most relevant components of the base excision repair system, and repair single-stranded DNA breaks, thus maintaining genome stability [12]. Additionally, PARP-1 and PARP-2 also participate in other biological functions such as angiogenesis and transcription [12,13], apoptosis of oxidative-stress related pathologies [14-16], and regulation of the immune response [11,12]. On the other hand, an increased activity or overexpression of PARP-1 and -2 may also induce cellular damage by depleting the ATP stores of cells in several conditions [17-20] or by altering the mechanisms of DNA repair, leading to tumorogenesis of several cancer types [12,21-24]. Therefore, the role of PARP-1 and PARP-2 in cells is two-fold: while they play a critical role in DNA repair, they may also favor carcinogenesis and tumor progression [12,21-25]. In line with the latter, PARP-1 overexpression was also shown to correlate with poor survival of patients with breast cancer [26].

Pharmacological inhibitors of PARP-1 and -2 were also demonstrated to be novel therapeutic targets for the treatment of several cancer types including LC [12,21-24,27-31]. Furthermore, the association of PARP inhibitors with cisplatin also showed to have additive effects on the treatment of LC as well as cervical, liver, and testicular cancers [27,28,30-32].

The precise mechanisms whereby PARP-1 and -2 inhibitors may reduce tumor size and growth remain to be fully understood.

Oxidative stress, defined as the imbalance between oxidant production and antioxidant activity in favor of the former is involved in the pathophysiology of a wide range of acute and chronic conditions including LC [33-36]. For instance, several mechanisms led to increased oxidative stress in LC tumorogenesis, resulting in the accumulation of reactive oxygen species (ROS) such as hydroxyl radicals and superoxide anion [35,37]. Besides, oxidative stress also triggers several responses in cells that may trigger autophagy [38,39] and cell death [40]. Enhanced oxidative stress also induced DNA damage in tumor cells, which involved the activation of PARP-1 and PARP-2 molecules [15,41], and miR-223 targets PARP-1 expression in cancer [42] and other conditions [43]. Collectively, these mechanisms it could be used as a potential target mechanism in cancer therapy. Moreover, overactivation of PARP-1 through increased oxidative stress was also shown to promote apoptosis and necrosis in cells [44,45]. Recent evidence also indicates that PARP-1 activation favors autophagy through enhanced oxidative stress in in vitro models [46,47]. Unpublished observations from our group have recently shown that levels of several markers of oxidative stress were increased in the subcutaneous tumors of lung adenocarcinoma cells in mice. Additionally, the size of the tumors was significantly reduced and several markers of tumor growth were decreased in mice that were genetically deficient for either PARP-1 or -2 bearing the same lung adenocarcinoma [48].

On the basis of these observations, we hypothesized that inhibition of either PARP-1 or -2 expressions in the host animals may influence tumor burden through several biological mechanisms such as redox imbalance (increased oxidative stress and/or reduced antioxidants and several cell regulators), autophagy, and apoptosis in the wild type lung adenocarcinoma cells. We reasoned that as it happens in patients receiving anticancer therapies, the host is likely to play a relevant role in tumor growth and progression regardless of the cancer

microenvironment and cell differentiation degree [49]. Accordingly, the main objectives in the current investigation were to assess in the lung adenocarcinoma tumors of Parp-$1^{-/-}$ and Parp-$2^{-/-}$ mice, the levels of oxidative stress, antioxidant enzymes, apoptosis, autophagy, and cell proliferation rates compared to tumors in wild type (WT) animals.

2. METHODS (See additional information on all the methodologies in the online supplementary material)

2.1 Animal experiments

2.1.1 Tumor. The LP07 cell line derives from the P07 lung tumor, which spontaneously arose in the lungs of BALB/c mice [50]. Moreover, one month after tumor transplantation, all animals developed lung metastasis and spleen enlargement without affecting other organs [36].

*2.1.2 Mice***.** BALB/c mice (2 months old, 20 g average weight) were obtained from Harlan *Interfauna Ibérica SL* (Barcelona, Spain). Parp-$1^{-/-}$ and Parp-$2^{-/-}$ mice (strain 129/Sv x C57BL/6), kindly provided by Dr. de Murcia [51] (Strasbourg, France), were backcrossed on BALB/c background for twelve generations. Genotyping was performed by PCR analysis of DNA from the tail vein as previously described [52]. All experiments were performed in 2 month's old (weight ~20g) female mice, on a BALB/c background.

2.1.3 Experimental design and Ethics. In all experimental groups, LP07 viable cells ($4 \cdot 10^5$) resuspended in 0.2 mL minimal essential media (MEM) were subcutaneously inoculated in the left flank of female BALB/c mice on day 1 and were studied for a period of one month. This was a controlled study designed in accordance with the ethical regulations on animal experimentation (EU 2010/63 CEE, *Real Decreto* 53/2013 BOE 34, Spain) at *Parc de Recerca Biomèdica de Barcelona* (PRBB) and the European Convention for the Protection of Vertebrate Animals Used for Experimental and Other Scientific Purposes (1986). All animal

experiments were approved by the Animal Research Committee at PRBB (protocol number EBP-09-1228).

2.2 In vivo measurements in the mice

Body weight and food intake were measured every day during the 30 days of the study period. Moreover, food and water were supplied ad libitum for the entire duration of the study protocol.

2.3 Sacrifice and sample collection

On day 30 post-inoculation of LP07 tumor cells, animals from all experimental groups were sacrificed immediately after an intraperitoneal injection of 0.1 mL sodium pentobarbital (60 mg/Kg). The subcutaneous tumors were obtained subsequently afterwards. In all mice, tumor weights were determined using a high-precision scale. Frozen tumors were used for immunoblotting techniques, while paraffin-embedded tumors were used for immunohistochemical experiments.

2.4 Tumor biology analyses

2.4.1 Immunoblotting of 1D electrophoresis. Protein levels of the different molecular markers and loading controls (Figures E1-E3) analyzed in the current investigation were evaluated according to methodologies published elsewhere [53].

2.4.2 Immunohistochemistry. In the tumor specimens from all groups, the cell proliferation marker ki-67 was identified on the three-micrometer tumor paraffin-embedded sections using an specific antibody and immunohistochemical procedures as previously described in our group [36]. In addition, the number of positively stained nuclei for Ki-67 was counted in tumors from all animal groups. Data are expressed as the percentage of positively-stained nuclei in each tumor from the three experimental groups of mice.

*2.4.3 RNA isolation***.** Total RNA was first isolated from snap-frozen tumors using the Trizol reagent following the manufacturer's protocol (Life technologies, Carlsbad, CA, USA). Total

RNA concentrations were determined spectrophotometrically using the NanoDrop 1000 (Thermo Scientific, Waltham, MA, USA).

2.4.4 MicroRNA reverse transcription (RT). MicroRNA RT was performed using TaqMan microRNA assays (Life Technologies) following the manufacturer's instructions.

2.4.5 Quantitative real time-PCR amplification (qRT-PCR). TaqMan based qPCR reactions were performed using the ABI PRISM 7900HT Sequence Detector System (Applied BioSystems, Foster City, CA, USA) together with a commercially available predesigned microRNA assay, primers, and probes (Tables 1 and 2), and published methodologies were followed [48].

2.5 Statistical analyses

All statistical analyses were performed using the software Statistical Package for the Social Sciences (SPSS) 15.0 (SPSS Inc, Chicago, IL, USA). Results are presented as median and interquartile ranges in the tables and as standard box plots with median (25th and 75th percentiles) and whiskers at minimum and maximum values in the graphs as precisely indicated by the expert statistician (Mr. Mojal). Comparisons of the different variables between LC-WT mice (control group) and either LC-Parp-1$^{-/-}$ or LC-Parp-2$^{-/-}$ mice were assessed using the non-parametric U Mann-Whitney test. Statistical significance was established at $P \leq 0.05$.

3. RESULTS

3.1 Physiologic characteristics of mice

At the end of the study period (day 30), WT animals bearing the lung adenocarcinoma tumors exhibited a significant reduction in body weight gain (Table 3). However, in LC-Parp-1$^{-/-}$ and LC-Parp-2$^{-/-}$ animals, body weight gain significantly increased compared to LC-WT (Table 3). Importantly, the expression of both PARP-1 and PARP-2 was confirmed in the

subcutaneous tumors of all experimental groups of mice (LC-WT, LC-Parp-1$^{-/-}$ and LC-Parp-2$^{-/-}$, Figures E2A and E2B). At the end of the study period, the size of the subcutaneous tumors, as measured by weight, was significantly reduced in both LC-Parp-1$^{-/-}$ and LC-Parp-2$^{-/-}$ mice compared to LC-WT (Table 3). The percentage of Ki-67 positively-stained nuclei, as a marker of tumor proliferation rate, was significantly decreased in LC-Parp-1$^{-/-}$ and LC-Parp-2$^{-/-}$ groups compared to LC-WT control animals (Table 3 and Figures 1A-1C).

3.2 Redox balance markers

3.2.1 Oxidative stress markers. No significant differences were found in total protein tyrosine nitration levels in the tumors between either LC-Parp-1$^{-/-}$ or LC-Parp-2$^{-/-}$ mice and LC-WT animals (Figure 2A and Figure E4). However, total MDA-protein adduct levels were significantly increased in the tumors of both LC-Parp-1$^{-/-}$ and LC-Parp-2$^{-/-}$ mice compared to LC-WT animals (Figures 2B and E5).

3.2.2 Antioxidant enzymes. Compared to LC-WT animals, protein levels of mitochondrial SOD2 and cytosolic SOD1 were significantly decreased in the tumors of LC-Parp-1$^{-/-}$ mice, but not in those of LC-Parp-2$^{-/-}$ (Figures 3A, 3B, E6, and E7, respectively). Catalase protein levels were significantly reduced in the tumors of both LC-Parp-2$^{-/-}$ and LC-Parp-1$^{-/-}$ rodents compared to LC-WT animals (Figures 3C and E8).

3.3 Apoptosis and autophagy markers

Bax protein levels were increased in the tumors of both LC-Parp-1$^{-/-}$ and LC-Parp-2$^{-/-}$ mice compared to LC-WT animals (Figures 4A and E9). The content of the antiapoptotic bcl-2 significantly decreased in the tumors of LC-Parp-1$^{-/-}$ and in LC-Parp-2$^{-/-}$ mice compared to LC-WT rodents (Figures 4B and E10). Interestingly, autophagy, as measured by the ratio of LC3-II to LC3-I protein content, was increased in the tumors of both LC-Parp-1$^{-/-}$ and LC-Parp-2$^{-/-}$ mice compared to LC-WT animals (Figures 5A and E11). No significant differences were found in sirtuin-1 protein levels in the tumors between LC-WT mice and either LC-Parp-1$^{-/-}$ or LC-Parp-2$^{-/-}$ animals (Figures 5B and E12).

3.4 Signaling regulators: expression of miR-223, NFATc-2 and HIF-1α

Expression of miR-223 was significantly decreased in the tumors of both LC-Parp-1$^{-/-}$ and LC-Parp-2$^{-/-}$ mice compared to LC-WT animals (Figure 6A). The expression of nuclear factor of activated T cells (NFAT)c-2 was significantly reduced only in the tumors of LC-Parp-1$^{-/-}$ rodents compared to LC-WT mice (Figure 6B). Nevertheless, no significant differences in hypoxia-induced factor (HIF)-1α expression were observed in the tumors of the different study groups of mice (Figure 6C).

4. DISCUSSION

The main findings in the current investigation were that in the subcutaneous WT tumors of Parp-1$^{-/-}$ and Parp-2$^{-/-}$ mice compared to those analyzed in the WT animals: 1) tumor burden, as measured by weight, and cell proliferation rates were decreased; 2) oxidative stress levels were greater, whereas those of the major antioxidant enzymes were lower, especially those of catalase; 3) tumor apoptosis and autophagy levels were significantly increased, and 4) expression of miR-223 and NFATc-2 was decreased (the latter only in LC-Parp-1$^{-/-}$ rodents). Furthermore, whole body weight gain at the end of the study period also improved in Parp-1$^{-/-}$ and Parp-2$^{-/-}$ mice compared to the WT animals. These findings confirm the study hypothesis to a great extent.

Specific genetic deletions of PARP-1 and PARP-2 in the host mice induced a reduction in tumor growth as well as a decrease in cell proliferation, as measured by the ki-67 marker. In line with these results, in lung cancer xenografts, the combination of radiotherapy with PARP-1 inhibitors also promoted a tumor growth delay [54,55] and a reduction of Ki-67 proliferation rates [54]. In addition, in a recent study, the combination of selective epidermal growth factor receptor (EGFR) and PARP-1 inhibitors also blocked tumor growth in ovarian cancer xenografts [56]. Moreover, the suppression of PARP-1 activity also resulted in a reduction of primary prostate tumor cell proliferation [25].

Interestingly, PARP-1 and PARP-2 seem to have important roles in DNA repair in response to oxidative stress [15,41]. In the current investigation, oxidative stress, as measured by MDA-protein adducts levels, was increased in the tumors of Parp-1$^{-/-}$ and LC-Parp-2$^{-/-}$ mice compared to those detected in the WT animals. Importantly, the levels of the potent antioxidants catalase were significantly reduced in the tumors of both Parp-1$^{-/-}$ and LC-Parp-2$^{-/-}$ animals along with those of SOD1 and SOD2 in the former mice compared to levels observed in the subcutaneous tumors of the WT rodents. Taken together, these findings suggest that the absence of either PARP-1 or PARP-2 expression and activity in the host mice may induce a downregulation of major antioxidant mechanisms such as catalase and, to lesser extent SODs, in the WT tumors containing lung adenocarcinoma cells. These are interesting findings that demonstrate the relevance of the status of the host in the progression and burden of WT tumors inoculated in the animals. In fact, these findings are similar to what happens in humans who take anticancer drugs, which also exert effects on the patients and the target tumors.

These findings are in agreement with another study in which inhibition of PARP activity in HT22 tumor cells increased oxidative stress markers as quantified by protein carbonyls and oxidized DNA [41]. Moreover, recent data from our group (unpublished observations) and others [57] have shown a significant reduction in levels of the antioxidant catalase in tumor lesions of patients with several cancer types including LC. Indeed, the decrease in catalase in this investigation was suggested to be a potential biomarker for lung cancer progression in the patients [57]. In addition, a substantial decrease in several oxidative stress markers was also shown in the lung adenocarcinoma tumors of WT mice treated with antioxidants (unpublished observations).

The precise mechanisms whereby the absence of PARP-1 and -2 may induce a decrease in antioxidant expression in this in vivo model will be the focus of future research. Nonetheless, in view of the current findings and previous observations [58,59] on the

potential role of PARP in the modulation of oxidant production and antioxidant activity, it could be assumed that PARP-1 and -2 genetic inhibition in the mice may have antioxidant activity that could induce a downregulation of antioxidant enzymes such as catalase and SODs within the tumor cells. In fact, pharmacological PARP inhibitors showed antioxidant activity through directly scavenging oxidant production in vitro [58]. In keeping with, in another study [59], overexpression of SODs was shown to prevent PARP expression and vice versa of neuronal cell death in a model of severe hypoglycemia. Collectively, it is possible to conclude from all the reported findings that PARP activity regulates the expression of major antioxidant systems in cells (SODs and catalase), thus inducing modifications in final oxidative stress balance that could be a target for anticancer treatment.

Importantly, oxidative stress also triggers different responses in cells such as cell death, e.g. apoptosis, and autophagy [60]. In the present study, the proapoptotic marker bax was increased, whereas levels of the anti-apoptotic bcl-2 were lower in the subcutaneous tumors of LC-Parp-1$^{-/-}$ and LC-Parp-2$^{-/-}$ mice than in tumors of the WT animals. These results suggest an increase in apoptotic events of tumor cells in Parp-1$^{-/-}$ and Parp-2$^{-/-}$ cancer bearing animals, which may partly account for the reduced tumor burden detected in these mice. Interestingly, such findings are also in line with previous studies, in which PARP-1 inhibitors were shown to induce cell death through apoptotic mechanisms in lung cancer cell lines [54,61]. Moreover, in one of these studies [54], levels of apoptosis enhanced as a result of PARP-1 inhibition in lung tumor xenografts exposed to radiotherapy. Other investigations have also shown an induction of apoptosis in response to PARP inhibitors in several tumor cell types such as malignant gliomas, HeLa, and myeloid leukemia [62-64].

In the current investigation, levels of the autophagy key regulator LC3-I/LC3-II were increased in the tumors of Parp-1$^{-/-}$ and Parp-2$^{-/-}$ mice compared to those detected in the tumors of the WT animals. Hence, it can be assumed that increased autophagy levels induced by PARP-1 and -2 genetic deletions may partly account for the reduced tumor burden

observed in the knockout animals compared to those in the WT mice. Interestingly, the current study findings are also in agreement with those encountered in a previous investigation, in which PARP-1 and PARP-2 inhibitors reduced tumor burden of ovarian cancer xenografts [56] and irradiated lung cancer cell lines [54] through the enhancement of autophagy.

The deacetylase enzyme sirtuin-1 may regulate upstream the LC3 pathway, thus playing a role in autophagy [65]. However, in the current study, protein levels of sirtuin-1 were found not to differ significantly in the lung adenocarcinoma tumors between WT and either Parp-$1^{-/-}$ or LC-Parp-$2^{-/-}$ mice. As the activation of sirtuin-1 requires the phosphorylation of several upstream molecules and cyclins [66], it is likely that this process may have not taken place in the tumor cells of the animals. Interestingly, PARP-1 inhibition was shown to induce a decrease in sirtuin-1 levels in fibroblasts exposed to cigarette smoke [67]. However, greater sirtuin-1 levels were shown in Parp-$1^{-/-}$and in Parp-$2^{-/-}$ mouse muscles in response to PARP inhibition [68,69]. Therefore, the implications of sirtuin-1 in PARP-1 and PARP-2 inhibition are still controversial and will be further elucidated in future research.

Another interesting finding was the downregulation observed in the expression of miR-223 in the tumors of both Parp-$1^{-/-}$ and LC-Parp-$2^{-/-}$ mice compared to wild type animals. Indeed, miR-223 has been recently shown to regulate PARP-1 expression in a model of pulmonary hypertension [43]. Furthermore, miR-223 was also shown to downregulate PARP-1 expression in patients with esophageal adenocarcinoma, and this mechanism was directly involved in the increased sensitivity of the cancer cells to chemotherapy [42]. Collectively, these findings suggest the existence of a negative feedback loop between PARP expression and that of miR-223 in adenocarcinoma that could account for the lack of response of PARP-1 inhibitors in certain cancers. Interestingly, another relevant finding was the significant downregulation of NFATc-2 detected in the tumors of Parp-$1^{-/-}$ mice, but not in those of Parp-$2^{-/-}$ animals compared to wild type rodents. These findings are in agreement with those

previously reported, in which PARP-1 activation was shown to upregulate the expression of several signaling molecules including NFATc-2 and HIF-1 alpha in pulmonary hypertension [70]. Taken together, it would be possibly suggested that another feedback loop may also exist between PARP-1 and NFATc-2 expressions in this model of adenocarcinoma.

Finally, it should also be discussed that cell growth and progression, as measured by ki-67 marker, were significantly reduced in the tumors of Parp-$1^{-/-}$and in Parp-$2^{-/-}$ mice compared to levels detected in the tumors of the WT animals. It is likely that cell cycle arrest as a result of altered expression of cyclins, e.g. cyclin D1, may account for the lower levels of ki-67 detected in the tumors of mice deficient in either PARP-1 or PARP-2 protein expression as shown to occur in other models in response to PARP inhibitors [21].

4.1 Study limitations

In the study, tumor weights were only measured on day 30 of the study protocol, when all animals were sacrificed. Nevertheless, we believe that this is not a major limitation, since tumors were monitored and obtained under identical experimental conditions in the three experimental groups of mice.

4.2 Conclusions

We conclude from this study that PARP-1 and -2 genetic deletions in the host mice induced a significant reduction in tumor burden most likely through alterations in redox balance and signaling pathways (decreased antioxidant enzymes, increased oxidative stress, and downregulated expression of miR-223 and NFATc-2), which in turn led to increased apoptosis and autophagy. Furthermore, tumor progression was also reduced probably as a result of cell cycle arrest induced by PARP-1 and -2 inhibition in the host mice. Taken together, these results point towards the relevance of the host status in tumor biology, at least in this experimental model of lung adenocarcinoma in mice. Future research will shed light on the effects of selective pharmacological inhibitors of PARP-1 and PARP-1 in the host and

tumor burden of mouse models of LC that could be eventually applied in actual clinical settings.

5. ACKNOWLEDGMENTS

The authors are thankful to Dr. Juan Martin-Caballero, Dr. Clara Fermoselle, MSs Alba Chacon-Cabrera, and Mr. Francisco Sanchez for their help with part of the animal experiments and biology analyses, to Ms. Coral Ampurdanes for her contribution to mouse genotyping, and to Mr. Sergio Mojal for his professional advice with the statistical analyses and data presentation. The study has been funded by *Instituto de Salud Carlos-III*: CIBERES, FIS 11/02029, FIS 14/00713 and Fundació La Marató de TV3: 2013-4130.

Editorial support: None to declare.

Reference List

[1] A. Jemal, F. Bray, M. M. Center, J. Ferlay, E. Ward, and D. Forman, Global cancer statistics, CA Cancer J. Clin., 61 (2011) 69-90.

[2] R. Siegel, J. Ma, Z. Zou, and A. Jemal, Cancer statistics, 2014, CA Cancer J. Clin., 64 (2014) 9-29.

[3] J. Ellis, The impact of lung cancer on patients and carers, Chron. Respir. Dis., 9 (2012) 39-47.

[4] C. Reddy, D. Chilla, and J. Boltax, Lung cancer screening: a review of available data and current guidelines, Hosp. Pract. (1995.), 39 (2011) 107-112.

[5] A. J. Alberg, J. G. Ford, and J. M. Samet, Epidemiology of lung cancer: ACCP evidence-based clinical practice guidelines (2nd edition), Chest, 132 (2007) 29S-55S.

[6] A. J. Alberg, M. V. Brock, J. G. Ford, J. M. Samet, and S. D. Spivack, Epidemiology of lung cancer: Diagnosis and management of lung cancer, 3rd ed: American College of Chest Physicians evidence-based clinical practice guidelines, Chest, 143 (2013) e1S-29S.

[7] G. J. Freixinet and P. M. Rodriguez Suarez, Morbidity, mortality and survival after surgery for lung cancer, Arch. Bronconeumol., 51 (2015) 211-212.

[8] E. Monso, L. M. Montuenga, C. J. Sanchez de, and C. Villena, Biological Marker Analysis as Part of the CIBERES-RTIC Cancer-SEPAR Strategic Project on Lung Cancer, Arch. Bronconeumol., (2015).

[9] P. Sanchez-Salcedo, J. Berto, J. P. de-Torres, A. Campo, A. B. Alcaide, G. Bastarrika, J. C. Pueyo, A. Villanueva, J. I. Echeveste, M. D. Lozano, M. J. Garcia-Velloso, L. M. Seijo, J. Garcia, W. Torre, M. J. Pajares, R. Pio, L. M. Montuenga, and J. J. Zulueta, Lung cancer screening: fourteen year experience of the Pamplona early detection program (P-IELCAP), Arch. Bronconeumol., 51 (2015) 169-176.

[10] M. Rodriguez, M. T. Gomez Hernandez, N. M. Novoa, J. L. Aranda, M. F. Jimenez, and G. Varela, Poorer Survival in Stage IB Lung Cancer Patients After Pneumonectomy, Arch. Bronconeumol., 51 (2015) 223-226.

[11] A. Burkle and L. Virag, Poly(ADP-ribose): PARadigms and PARadoxes, Mol. Aspects Med., 34 (2013) 1046-1065.

[12] J. Yelamos, J. Farres, L. Llacuna, C. Ampurdanes, and J. Martin-Caballero, PARP-1 and PARP-2: New players in tumour development, Am. J. Cancer Res., 1 (2011) 328-346.

[13] J. Yelamos, V. Schreiber, and F. Dantzer, Toward specific functions of poly(ADP-ribose) polymerase-2, Trends Mol. Med., 14 (2008) 169-178.

[14] J. I. Diaz-Hernandez, S. Moncada, J. P. Bolanos, and A. Almeida, Poly(ADP-ribose) polymerase-1 protects neurons against apoptosis induced by oxidative stress, Cell Death. Differ., 14 (2007) 1211-1221.

[15] X. Luo and W. L. Kraus, On PAR with PARP: cellular stress signaling through poly(ADP-ribose) and PARP-1, Genes Dev., 26 (2012) 417-432.

[16] S. W. Yu, S. A. Andrabi, H. Wang, N. S. Kim, G. G. Poirier, T. M. Dawson, and V. L. Dawson, Apoptosis-inducing factor mediates poly(ADP-ribose) (PAR) polymer-induced cell death, Proc. Natl. Acad. Sci. U. S. A, 103 (2006) 18314-18319.

[17] H. C. Ha and S. H. Snyder, Poly(ADP-ribose) polymerase is a mediator of necrotic cell death by ATP depletion, Proc. Natl. Acad. Sci. U. S. A, 96 (1999) 13978-13982.

[18] R. Kiefmann, K. Heckel, M. Doerger, S. Schenkat, C. Kupatt, M. Stoeckelhuber, J. Wesierska-Gadek, and A. E. Goetz, Role of PARP on iNOS pathway during endotoxin-induced acute lung injury, Intensive Care Med., 30 (2004) 1421-1431.

[19] R. Vaschetto, J. W. Kuiper, S. R. Chiang, J. J. Haitsma, J. W. Juco, S. Uhlig, F. B. Plotz, C. F. Della, H. Zhang, and A. S. Slutsky, Inhibition of poly(adenosine diphosphate-ribose) polymerase attenuates ventilator-induced lung injury, Anesthesiology, 108 (2008) 261-268.

[20] J. Zheng, K. Devalaraja-Narashimha, K. Singaravelu, and B. J. Padanilam, Poly(ADP-ribose) polymerase-1 gene ablation protects mice from ischemic renal injury, Am. J. Physiol Renal Physiol, 288 (2005) F387-F398.

[21] P. De, Y. Sun, J. H. Carlson, L. S. Friedman, B. R. Leyland-Jones, and N. Dey, Doubling down on the PI3K-AKT-mTOR pathway enhances the antitumor efficacy of PARP inhibitor in triple negative breast cancer model beyond BRCA-ness, Neoplasia., 16 (2014) 43-72.

[22] H. Sui, C. Shi, Z. Yan, and H. Li, Combination of erlotinib and a PARP inhibitor inhibits growth of A2780 tumor xenografts due to increased autophagy, Drug Des Devel. Ther., 9 (2015) 3183-3190.

[23] K. S. Tewari, R. N. Eskander, and B. J. Monk, Development of Olaparib for BRCA-Deficient Recurrent Epithelial Ovarian Cancer, Clin. Cancer Res., (2015).

[24] R. van der Noll, S. Marchetti, N. Steeghs, J. H. Beijnen, M. W. Mergui-Roelvink, E. Harms, H. Rehorst, G. S. Sonke, and J. H. Schellens, Long-term safety and anti-tumour activity of olaparib monotherapy after combination with carboplatin and paclitaxel in patients with advanced breast, ovarian or fallopian tube cancer, Br. J. Cancer, (2015).

[25] M. J. Schiewer, J. F. Goodwin, S. Han, J. C. Brenner, M. A. Augello, J. L. Dean, F. Liu, J. L. Planck, P. Ravindranathan, A. M. Chinnaiyan, P. McCue, L. G. Gomella, G. V. Raj, A. P. Dicker, J. R. Brody, J. M. Pascal, M. M. Centenera, L. M. Butler, W. D. Tilley, F. Y. Feng, and K. E. Knudsen, Dual roles of PARP-1 promote cancer growth and progression, Cancer Discov., 2 (2012) 1134-1149.

[26] F. Rojo, J. Garcia-Parra, S. Zazo, I. Tusquets, J. Ferrer-Lozano, S. Menendez, P. Eroles, C. Chamizo, S. Servitja, N. Ramirez-Merino, F. Lobo, B. Bellosillo, J. M.

Corominas, J. Yelamos, S. Serrano, A. Lluch, A. Rovira, and J. Albanell, Nuclear PARP-1 protein overexpression is associated with poor overall survival in early breast cancer, Ann. Oncol., 23 (2012) 1156-1164.

[27] D. Davar, J. H. Beumer, L. Hamieh, and H. Tawbi, Role of PARP inhibitors in cancer biology and therapy, Curr. Med. Chem., 19 (2012) 3907-3921.

[28] P. Domagala, T. Huzarski, J. Lubinski, K. Gugala, and W. Domagala, PARP-1 expression in breast cancer including BRCA1-associated, triple negative and basal-like tumors: possible implications for PARP-1 inhibitor therapy, Breast Cancer Res. Treat., 127 (2011) 861-869.

[29] J. M. Lee, J. A. Ledermann, and E. C. Kohn, PARP Inhibitors for BRCA1/2 mutation-associated and BRCA-like malignancies, Ann. Oncol., 25 (2014) 32-40.

[30] Y. R. Lee, D. S. Yu, Y. C. Liang, K. F. Huang, S. J. Chou, T. C. Chen, C. C. Lee, C. L. Chen, S. H. Chiou, and H. S. Huang, New approaches of PARP-1 inhibitors in human lung cancer cells and cancer stem-like cells by some selected anthraquinone-derived small molecules, PLoS. One., 8 (2013) e56284.

[31] S. Postel-Vinay, I. Bajrami, L. Friboulet, R. Elliott, Y. Fontebasso, N. Dorvault, K. A. Olaussen, F. Andre, J. C. Soria, C. J. Lord, and A. Ashworth, A high-throughput screen identifies PARP1/2 inhibitors as a potential therapy for ERCC1-deficient non-small cell lung cancer, Oncogene, 32 (2013) 5377-5387.

[32] M. Rouleau, A. Patel, M. J. Hendzel, S. H. Kaufmann, and G. G. Poirier, PARP inhibition: PARP1 and beyond, Nat. Rev. Cancer, 10 (2010) 293-301.

[33] E. Barreiro, D. Sanchez, J. B. Galdiz, S. N. Hussain, and J. Gea, N-acetylcysteine increases manganese superoxide dismutase activity in septic rat diaphragms, Eur. Respir. J., 26 (2005) 1032-1039.

[34] E. Barreiro, V. I. Peinado, J. B. Galdiz, E. Ferrer, J. Marin-Corral, F. Sanchez, J. Gea, and J. A. Barbera, Cigarette smoke-induced oxidative stress: A role in chronic obstructive pulmonary disease skeletal muscle dysfunction, Am. J. Respir. Crit Care Med., 182 (2010) 477-488.

[35] E. Barreiro, C. Fermoselle, M. Mateu-Jimenez, A. Sanchez-Font, L. Pijuan, J. Gea, and V. Curull, Oxidative stress and inflammation in the normal airways and blood of patients with lung cancer and COPD, Free Radic. Biol. Med., 65 (2013) 859-871.

[36] A. Chacon-Cabrera, C. Fermoselle, A. J. Urtreger, M. Mateu-Jimenez, M. J. Diament, E. D. de Kier Joffe, M. Sandri, and E. Barreiro, Pharmacological strategies in lung cancer-induced cachexia: effects on muscle proteolysis, autophagy, structure, and weakness, J. Cell Physiol, 229 (2014) 1660-1672.

[37] A. Gupta, S. Srivastava, R. Prasad, S. M. Natu, B. Mittal, M. P. Negi, and A. N. Srivastava, Oxidative stress in non-small cell lung cancer patients after chemotherapy: association with treatment response, Respirology., 15 (2010) 349-356.

[38] G. Filomeni, Z. D. De, and F. Cecconi, Oxidative stress and autophagy: the clash between damage and metabolic needs, Cell Death. Differ., 22 (2015) 377-388.

[39] J. J. Jaboin, M. Hwang, and B. Lu, Autophagy in lung cancer, Methods Enzymol., 453 (2009) 287-304.

[40] M. M. Pore, T. J. Hiltermann, and F. A. Kruyt, Targeting apoptosis pathways in lung cancer, Cancer Lett., 332 (2013) 359-368.

[41] B. Catalgol, B. Wendt, S. Grimm, N. Breusing, N. K. Ozer, and T. Grune, Chromatin repair after oxidative stress: role of PARP-mediated proteasome activation, Free Radic. Biol. Med., 48 (2010) 673-680.

[42] M. M. Streppel, S. Pai, N. R. Campbell, C. Hu, S. Yabuuchi, M. I. Canto, J. S. Wang, E. A. Montgomery, and A. Maitra, MicroRNA 223 is upregulated in the multistep progression of Barrett's esophagus and modulates sensitivity to chemotherapy by targeting PARP1, Clin. Cancer Res., 19 (2013) 4067-4078.

[43] J. Meloche, G. M. Le, F. Potus, J. Vinck, B. Ranchoux, I. Johnson, F. Antigny, E. Tremblay, S. Breuils-Bonnet, F. Perros, S. Provencher, and S. Bonnet, miR-223 reverses experimental pulmonary arterial hypertension, Am. J. Physiol Cell Physiol, 309 (2015) C363-C372.

[44] S. A. Andrabi, N. S. Kim, S. W. Yu, H. Wang, D. W. Koh, M. Sasaki, J. A. Klaus, T. Otsuka, Z. Zhang, R. C. Koehler, P. D. Hurn, G. G. Poirier, V. L. Dawson, and T. M. Dawson, Poly(ADP-ribose) (PAR) polymer is a death signal, Proc. Natl. Acad. Sci. U. S. A, 103 (2006) 18308-18313.

[45] S. W. Yu, H. Wang, M. F. Poitras, C. Coombs, W. J. Bowers, H. J. Federoff, G. G. Poirier, T. M. Dawson, and V. L. Dawson, Mediation of poly(ADP-ribose) polymerase-1-dependent cell death by apoptosis-inducing factor, Science, 297 (2002) 259-263.

[46] J. A. Munoz-Gamez, J. M. Rodriguez-Vargas, R. Quiles-Perez, R. Aguilar-Quesada, D. Martin-Oliva, M. G. de, M. J. Menissier de, A. Almendros, A. M. Ruiz de, and F. J. Oliver, PARP-1 is involved in autophagy induced by DNA damage, Autophagy., 5 (2009) 61-74.

[47] J. M. Rodriguez-Vargas, M. J. Ruiz-Magana, C. Ruiz-Ruiz, J. Majuelos-Melguizo, A. Peralta-Leal, M. I. Rodriguez, J. A. Munoz-Gamez, M. R. de Almodovar, E. Siles, A. L. Rivas, M. Jaattela, and F. J. Oliver, ROS-induced DNA damage and PARP-1 are required for optimal induction of starvation-induced autophagy, Cell Res., 22 (2012) 1181-1198.

[48] A. Chacon-Cabrera, C. Fermoselle, I. Salmela, J. Yelamos, and E. Barreiro, MicroRNA expression and protein acetylation pattern in respiratory and limb muscles of Parp-1(-/-) and Parp-2(-/-) mice with lung cancer cachexia, Biochim. Biophys. Acta, 1850 (2015) 2530-2543.

[49] D. Tarin, Role of the host stroma in cancer and its therapeutic significance, Cancer Metastasis Rev., 32 (2013) 553-566.

[50] M. J. Diament, C. Garcia, I. Stillitani, V. M. Saavedra, T. Manzur, L. Vauthay, and S. Klein, Spontaneous murine lung adenocarcinoma (P07): A new experimental model to study paraneoplastic syndromes of lung cancer, Int. J. Mol. Med., 2 (1998) 45-50.

[51] J. M. de Murcia, C. Niedergang, C. Trucco, M. Ricoul, B. Dutrillaux, M. Mark, F. J. Oliver, M. Masson, A. Dierich, M. LeMeur, C. Walztinger, P. Chambon, and M. G. de, Requirement of poly(ADP-ribose) polymerase in recovery from DNA damage in mice and in cells, Proc. Natl. Acad. Sci. U. S. A, 94 (1997) 7303-7307.

[52] J. Corral, J. Yelamos, D. Hernandez-Espinosa, Y. Monreal, R. Mota, I. Arcas, A. Minano, P. Parrilla, and V. Vicente, Role of lipopolysaccharide and cecal ligation and puncture on blood coagulation and inflammation in sensitive and resistant mice models, Am. J. Pathol., 166 (2005) 1089-1098.

[53] C. Fermoselle, R. Rabinovich, P. Ausin, E. Puig-Vilanova, C. Coronell, F. Sanchez, J. Roca, J. Gea, and E. Barreiro, Does oxidative stress modulate limb muscle atrophy in severe COPD patients?, Eur. Respir. J., 40 (2012) 851-862.

[54] J. M. Albert, C. Cao, K. W. Kim, C. D. Willey, L. Geng, D. Xiao, H. Wang, A. Sandler, D. H. Johnson, A. D. Colevas, J. Low, M. L. Rothenberg, and B. Lu, Inhibition of poly(ADP-ribose) polymerase enhances cell death and improves tumor growth delay in irradiated lung cancer models, Clin. Cancer Res., 13 (2007) 3033-3042.

[55] J. M. Senra, B. A. Telfer, K. E. Cherry, C. M. McCrudden, D. G. Hirst, M. J. O'Connor, S. R. Wedge, and I. J. Stratford, Inhibition of PARP-1 by olaparib (AZD2281) increases the radiosensitivity of a lung tumor xenograft, Mol. Cancer Ther., 10 (2011) 1949-1958.

[56] H. Sui, C. Shi, Z. Yan, and H. Li, Combination of erlotinib and a PARP inhibitor inhibits growth of A2780 tumor xenografts due to increased autophagy, Drug Des Devel. Ther., 9 (2015) 3183-3190.

[57] A. Miar, D. Hevia, H. Munoz-Cimadevilla, A. Astudillo, J. Velasco, R. M. Sainz, and J. C. Mayo, Manganese superoxide dismutase (SOD2/MnSOD)/catalase and SOD2/GPx1 ratios as biomarkers for tumor progression and metastasis in prostate, colon, and lung cancer, Free Radic. Biol. Med., 85 (2015) 45-55.

[58] T. Kalai, M. Balog, A. Szabo, G. Gulyas, J. Jeko, B. Sumegi, and K. Hideg, New poly(ADP-ribose) polymerase-1 inhibitors with antioxidant activity based on 4-carboxamidobenzimidazole-2-ylpyrroline and -tetrahydropyridine nitroxides and their precursors, J. Med. Chem., 52 (2009) 1619-1629.

[59] S. W. Suh, A. M. Hamby, E. T. Gum, B. S. Shin, S. J. Won, C. T. Sheline, P. H. Chan, and R. A. Swanson, Sequential release of nitric oxide, zinc, and superoxide in hypoglycemic neuronal death, J. Cereb. Blood Flow Metab, 28 (2008) 1697-1706.

[60] P. Wyrsch, C. Blenn, J. Bader, and F. R. Althaus, Cell death and autophagy under oxidative stress: roles of poly(ADP-Ribose) polymerases and Ca(2+), Mol. Cell Biol., 32 (2012) 3541-3553.

[61] N. N. Gangopadhyay, J. D. Luketich, A. Opest, C. Visus, E. M. Meyer, R. Landreneau, and M. J. Schuchert, Inhibition of poly(ADP-ribose) polymerase (PARP) induces apoptosis in lung cancer cell lines, Cancer Invest, 29 (2011) 608-616.

[62] G. Karpel-Massler, F. Pareja, P. Aime, C. Shu, L. Chau, M. A. Westhoff, M. E. Halatsch, J. F. Crary, P. Canoll, and M. D. Siegelin, PARP inhibition restores extrinsic apoptotic sensitivity in glioblastoma, PLoS. One., 9 (2014) e114583.

[63] T. J. Gaymes, S. Shall, L. J. MacPherson, N. A. Twine, N. C. Lea, F. Farzaneh, and G. J. Mufti, Inhibitors of poly ADP-ribose polymerase (PARP) induce apoptosis of myeloid leukemic cells: potential for therapy of myeloid leukemia and myelodysplastic syndromes, Haematologica, 94 (2009) 638-646.

[64] C. Ethier, Y. Labelle, and G. G. Poirier, PARP-1-induced cell death through inhibition of the MEK/ERK pathway in MNNG-treated HeLa cells, Apoptosis., 12 (2007) 2037-2049.

[65] R. Huang, Y. Xu, W. Wan, X. Shou, J. Qian, Z. You, B. Liu, C. Chang, T. Zhou, J. Lippincott-Schwartz, and W. Liu, Deacetylation of nuclear LC3 drives autophagy initiation under starvation, Mol. Cell, 57 (2015) 456-466.

[66] A. Luna, M. I. Aladjem, and K. W. Kohn, SIRT1/PARP1 crosstalk: connecting DNA damage and metabolism, Genome Integr., 4 (2013) 6.

[67] J. W. Hwang, S. Chung, I. K. Sundar, H. Yao, G. Arunachalam, M. W. McBurney, and I. Rahman, Cigarette smoke-induced autophagy is regulated by SIRT1-PARP-1-dependent mechanism: implication in pathogenesis of COPD, Arch. Biochem. Biophys., 500 (2010) 203-209.

[68] P. Bai, C. Canto, H. Oudart, A. Brunyanszki, Y. Cen, C. Thomas, H. Yamamoto, A. Huber, B. Kiss, R. H. Houtkooper, K. Schoonjans, V. Schreiber, A. A. Sauve, M. J. Menissier-de, and J. Auwerx, PARP-1 inhibition increases mitochondrial metabolism through SIRT1 activation, Cell Metab, 13 (2011) 461-468.

[69] P. Bai, C. Canto, A. Brunyanszki, A. Huber, M. Szanto, Y. Cen, H. Yamamoto, S. M. Houten, B. Kiss, H. Oudart, P. Gergely, M. J. Menissier-de, V. Schreiber, A. A. Sauve, and J. Auwerx, PARP-2 regulates SIRT1 expression and whole-body energy expenditure, Cell Metab, 13 (2011) 450-460.

[70] J. Meloche, A. Pflieger, M. Vaillancourt, R. Paulin, F. Potus, S. Zervopoulos, C. Graydon, A. Courboulin, S. Breuils-Bonnet, E. Tremblay, C. Couture, E. D. Michelakis, S. Provencher, and S. Bonnet, Role for DNA damage signaling in pulmonary arterial hypertension, Circulation, 129 (2014) 786-797.

FIGURE LEGENDS

Figure 1: Representative examples of Ki-67 immunostaining in the subcutaneous tumor of LC-WT animals (panel A), LC- Parp-1$^{-/-}$ (panel B) and LC-Parp-2$^{-/-}$ mice (panel C). Positive Ki-67 nuclei are stained in brown color. Black arrows point towards Ki-67 positively-stained nuclei (in brown), while red arrows point towards Ki-67 negatively- stained nuclei (in purple).

Figure 2:

A) Optical densities in the box plots are expressed as optical densities of total protein tyrosine nitration levels in the subcutaneous tumors of LC mice. Standard box plots with median (25th and 75th percentiles) and whiskers at minimum and maximum values are depicted. No significant differences were found in total protein tyrosine nitration in LC-Parp-1$^{-/-}$ and LC-Parp-2$^{-/-}$ mice (N=6) compared to LC-WT rodents (N=9). Statistical significance is as follows: n.s.: non-significant between LC-WT group and LC-Parp-1$^{-/-}$ or LC-Parp-2$^{-/-}$ mice.

B) Optical densities in the box plots are expressed as optical densities of MDA-protein adduct levels in the subcutaneous tumors of LC mice. Standard box plots with median (25th and 75th percentiles) and whiskers at minimum and maximum values are depicted. Total MDA-protein adducts levels were significantly increased in both LC-Parp-1$^{-/-}$ and LC-Parp-2$^{-/-}$ animals (N=6) compared to LC-WT rodents (N=9). Statistical significance is as follows: *: $p<0.05$ and **: $p<0.01$ between LC-WT animals and either LC-Parp-1$^{-/-}$ or LC-Parp-2$^{-/-}$ mice.

Figure 3

A) Optical densities in the box plots are expressed as optical densities of SOD2 protein levels in the subcutaneous tumors of LC mice. Standard box plots with median (25th and 75th percentiles) and whiskers at minimum and maximum values are depicted.

SOD2 protein content was significantly decreased only in LC-Parp-1$^{-/-}$ animals (N=6) compared to LC-WT (N=9). Statistical significance is as follows: n.s.: non-significant and **: p<0.01 between LC-WT animals and LC-Parp-1$^{-/-}$ mice.

B) Optical densities in the box plots are expressed as optical densities of SOD1 protein levels in the subcutaneous tumors of LC mice. Standard box plots with median (25th and 75th percentiles) and whiskers at minimum and maximum values are depicted. SOD1 protein content was significantly decreased only in LC-Parp-1$^{-/-}$ animals (N=6) compared to LC-WT (N=9). Statistical significance is as follows: n.s.: non-significant and *: p <0.05 between LC-WT animals and LC-Parp-2$^{-/-}$ mice.

C) Optical densities in the box plots are expressed as optical densities of catalase protein levels in the subcutaneous tumors of LC mice. Standard box plots with median (25th and 75th percentiles) and whiskers at minimum and maximum values are depicted. Catalase protein content was significantly reduced in both LC-Parp-1$^{-/-}$ and LC-Parp-2$^{-/-}$ animals (N=6) compared to LC-WT rodents (N=9). Statistical significance is as follows: *: p <0.05 between LC-WT animals and either LC-Parp-1$^{-/-}$ or LC-Parp-2$^{-/-}$ mice.

Figure 4

A) Optical densities in the box plots are expressed as optical densities of bax protein levels in the subcutaneous tumors of LC mice. Standard box plots with median (25th and 75th percentiles) and whiskers at minimum and maximum values are depicted. Bax protein content was significantly increased in both LC-Parp-1$^{-/-}$ and LC-Parp-2$^{-/-}$ animals (N=6) compared to LC-WT rodents (N=9). Statistical significance is as follows: *: p <0.05 between LC-WT animals and either LC-Parp-1$^{-/-}$ or LC-Parp-2$^{-/-}$ mice.

B) Optical densities in the box plots are expressed as optical densities of bcl-2 protein levels in the subcutaneous tumors of LC mice. Standard box plots with median (25th and 75th percentiles) and whiskers at minimum and maximum values are depicted. Bcl-2 protein content was significantly decreased in both LC-Parp-$1^{-/-}$ and LC-Parp-$2^{-/-}$ animals (N=6) compared to LC-WT rodents (N=9). Statistical significance is as follows: *: $p < 0.05$ and **: $p < 0.01$ between LC-WT animals and either LC-Parp-$1^{-/-}$ or LC-Parp-$2^{-/-}$ mice.

Figure 5:

A) Optical densities in the box plots are expressed as optical densities of total LC3-II/LC3-I levels in the subcutaneous tumors of LC mice. Standard box plots with median (25th and 75th percentiles) and whiskers at minimum and maximum values are depicted. LC3-II/LC3-I protein content was significantly increased in both LC-Parp-$1^{-/-}$ and LC-Parp-$2^{-/-}$ animals (N=6) compared to LC-WT rodents (N=9). Statistical significance is as follows: *: $p < 0.05$ and ***: $p < 0.001$ between LC-WT animals and either LC-Parp-$1^{-/-}$ or LC-Parp-$2^{-/-}$ mice.

B) Optical densities in the box plots are expressed as optical densities of Sirtuin-1 (SIRT-1) protein levels in the subcutaneous tumors of LC mice. Standard box plots with median (25th and 75th percentiles) and whiskers at minimum and maximum values are depicted. No significant differences were found in SIRT-1 protein content in tumors between LC-WT mice (N=9) and LC-Parp-$1^{-/-}$ and LC-Parp-$2^{-/-}$ mice (N=6). Statistical significance is as follows: n.s.: non-significant between LC-WT animals and either LC-Parp-$1^{-/-}$ or LC-Parp-$2^{-/-}$ mice.

Figure 6

A) Relative miR-223 expression in the subcutaneous tumors of LC mice is shown in the box plots. Standard box plots with median (25th and 75th percentiles) and whiskers at minimum and maximum values are depicted. The expression of miR-223 was decreased in both LC-Parp-1$^{-/-}$ (N=9) and LC-Parp-2$^{-/-}$ animals (N=8) compared to LC-WT rodents (N=10). Statistical significance is as follows: *: $p < 0.05$ between LC-WT animals and either LC-Parp-1$^{-/-}$ or LC-Parp-2$^{-/-}$ mice.

B) Relative NFATc-2 expression in the subcutaneous tumors of LC mice is shown in the boxplots. Standard box plots with median (25th and 75th percentiles) and whiskers at minimum and maximum values are depicted. NFATc-2 expression was reduced in LC-Parp-1$^{-/-}$ rodents (N=9) compared to LC-WT mice (N=10). Statistical significance is as follows: **: $p < 0.01$ and n.s.: non-significant between LC-WT animals and either LC-Parp-1$^{-/-}$ or LC-Parp-2$^{-/-}$ mice.

C) Relative HIF-1α in the subcutaneous tumors of LC mice is shown in the boxplots. Standard box plots with median (25th and 75th percentiles) and whiskers at minimum and maximum values are depicted. No significant differences were found in HIF-1α expression between either LC-Parp-1$^{-/-}$ (N=9) or LC-Parp-2$^{-/-}$ mice (N=8) and LC-WT rodents (N=10). Statistical significance is as follows: n.s.: non-significant between LC-WT animals and either LC-Parp-1$^{-/-}$ or LC-Parp-2$^{-/-}$ mice.

Tables

Table 1 . MicroRNA assays used for the quantitative analyses of the target genes using real-time PCR.

Assay Name	Assay ID	miRBase accession number
hsa-miR-223	000526	MIMAT0002593;
		NCBI Accession number
U6 snRNA, housekeeping gene	001973	NR_004394

Abbreviations: ID, identification; hsa, homo sapiens; miR, microRNA; MIMAT, mature microRNA; snRNA, small nuclear RNA; and NR, non-coding RNA RefSeq database category.

Table 2 . Probes used for the quantitative analyses of the target genes using real-time PCR.

Gene Symbol	Assay ID	GeneBank accession number
NFATc-2	Mm01240677_m1	NM_001037177.2
HIF-1α	Mm00468869_m1	NM_010431.2
GAPDH	Mm99999915_g1	NM_001289726.1

Abbreviations: ID, identification; Mm, mus musculus; m1, multi-exonic gene assay does not detect genomic DNA; NM, mRNA RefSeq database category; NFATc-2, nuclear factor of activated T cells, cytoplasmic, calcineurin dependent 2 ; HIF-1α, hypoxia inducible factor 1, alpha subunit; GAPDH, glyceraldehyde-3-phosphate dehydrogenase; and g1, multi-exonic gene assay may detect genomic DNA if presenting the sample.

Tables

Table 3. Body weights and tumor size and growth in mice from all experimental groups at the end of the study period (30 days)

	LC-WT (N=9)	**LC-Parp-1$^{-/-}$** (N=6)	**LC-Parp-2$^{-/-}$** (N=6)
Body weight gain (%)	-4.77 (4.67)	+1.95 (3.00), **	+3.34 (7.01), *
Subcutaneous tumor weight (g)	1.89 (0.49)	1.13 (0.41), **	1.30 (0.39), *
Tumor weight loss (%)	NA	40.55	31.12
Ki-67 positively stained nuclei (%)	95 (4)	87 (3), **	88 (5), *

Variables are presented as median (interquartile ranges).
Statistical significance: *: p≤0.05, **: p≤0.01 between either LC-Parp-1$^{-/-}$ or LC-Parp-2$^{-/-}$ compared to LC-WT.
Definition of abbreviations: LC-WT: lung cancer wild type mice, LC-Parp-1$^{-/-}$: lung cancer Parp-1$^{-/-}$ mice, LC-Parp-2$^{-/-}$: lung cancer Parp-2$^{-/-}$ mice, NA: not applicable.

Figure

Click here to download high resolution image

M. Mateu-Jimenez *et al.* Figure 1

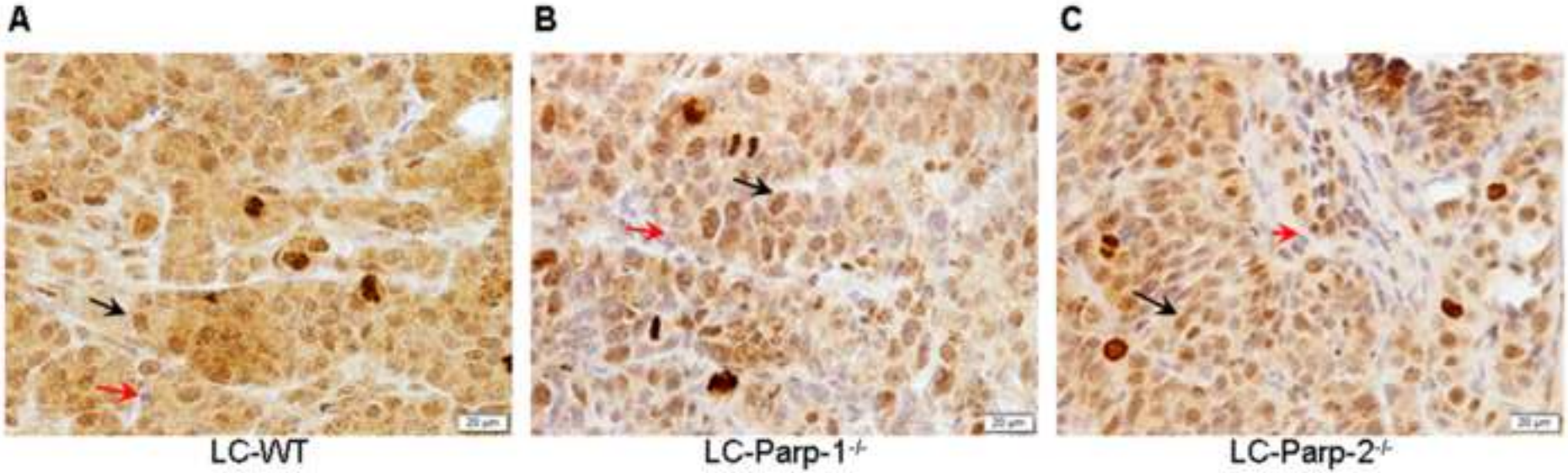

Figure

Click here to download high resolution image

M. Mateu-Jimenez *et al.* Figure 2

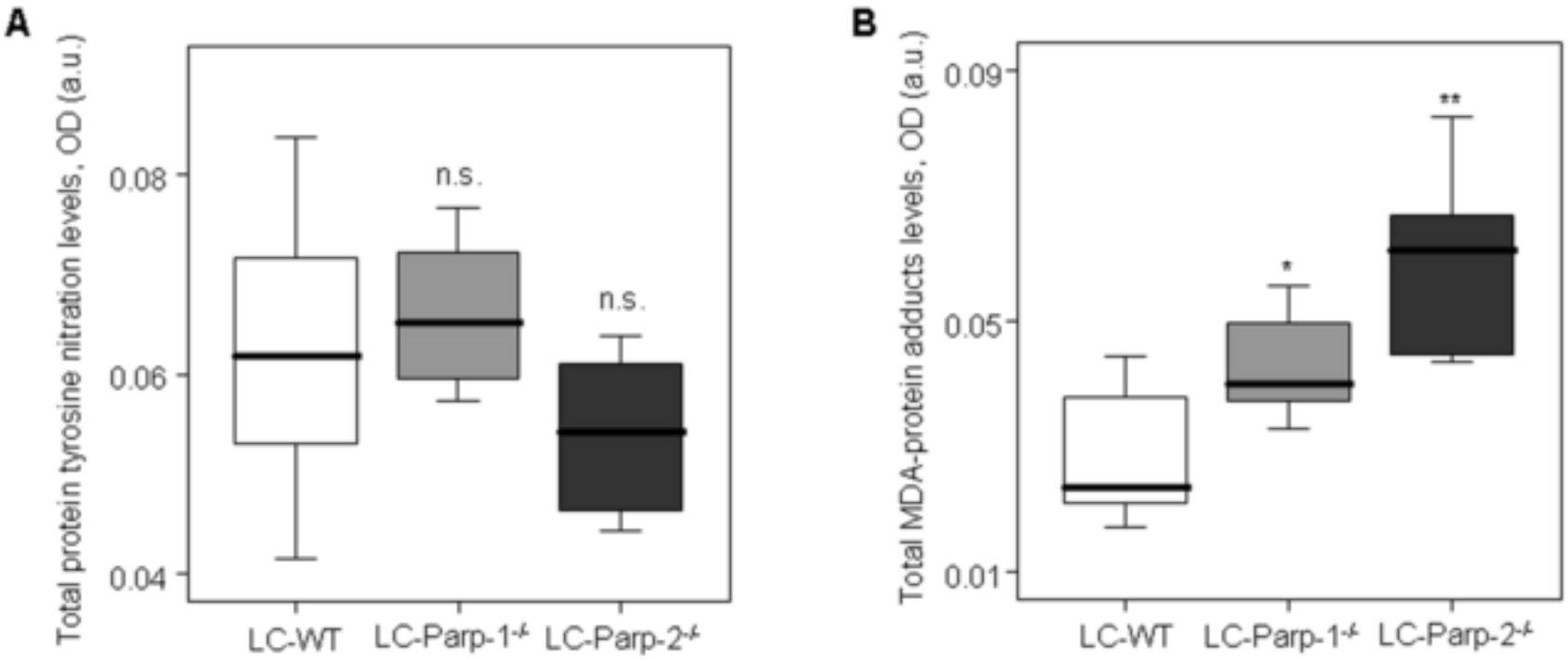

Figure

Click here to download high resolution image

M. Mateu-Jimenez *et al.* Figure 3

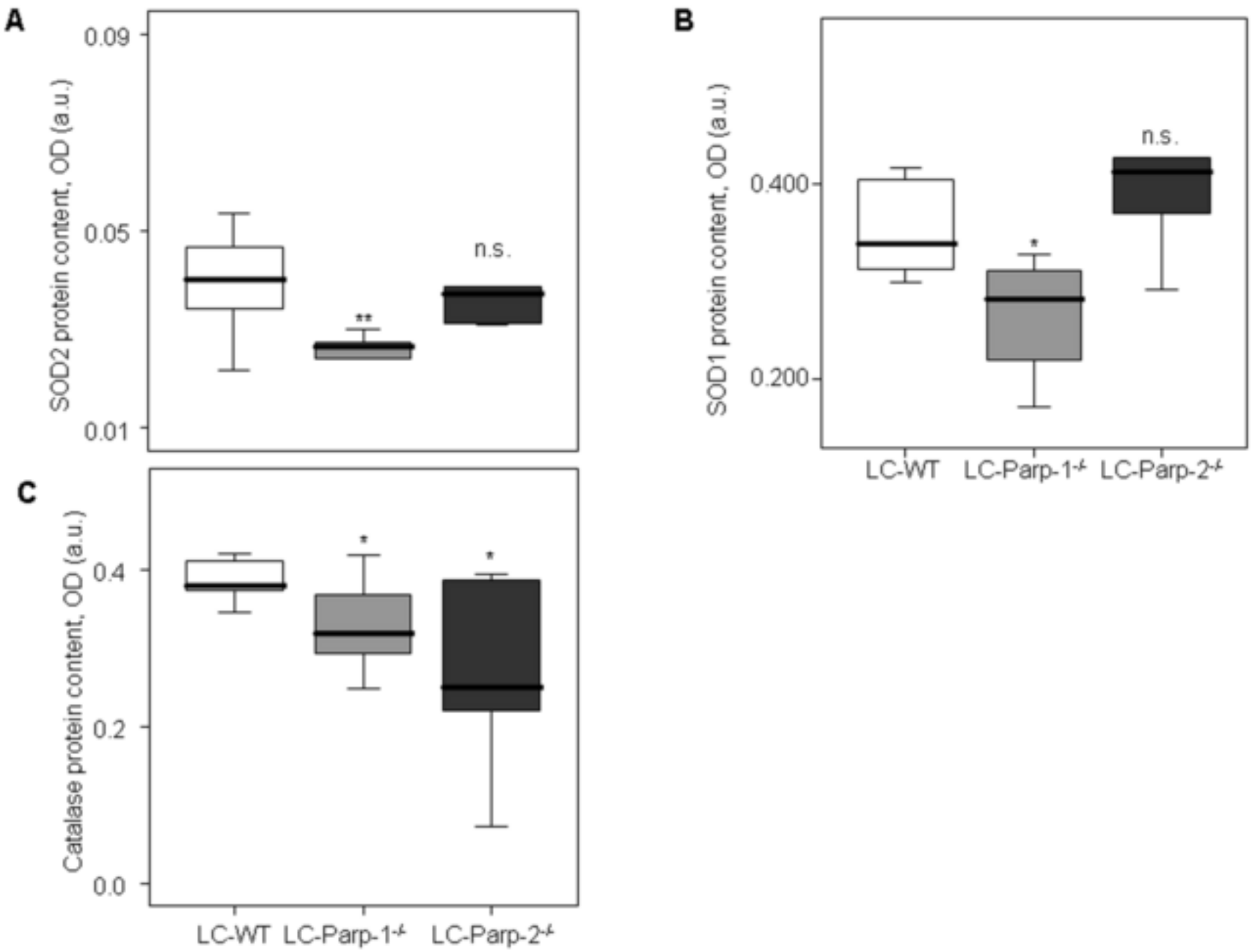

Figure

Click here to download high resolution image

M. Mateu-Jimenez *et al.* Figure 4

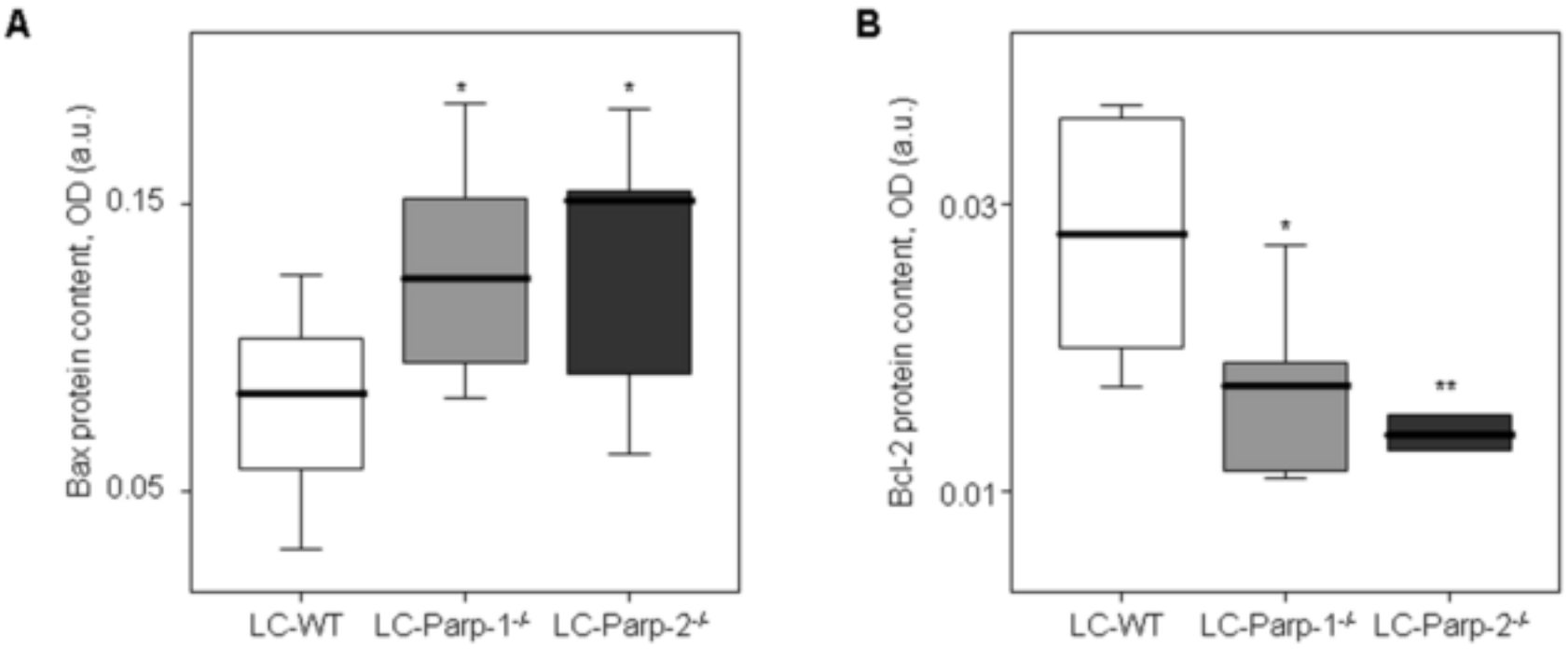

Figure
Click here to download high resolution image

M. Mateu-Jimenez *et al.* Figure 5

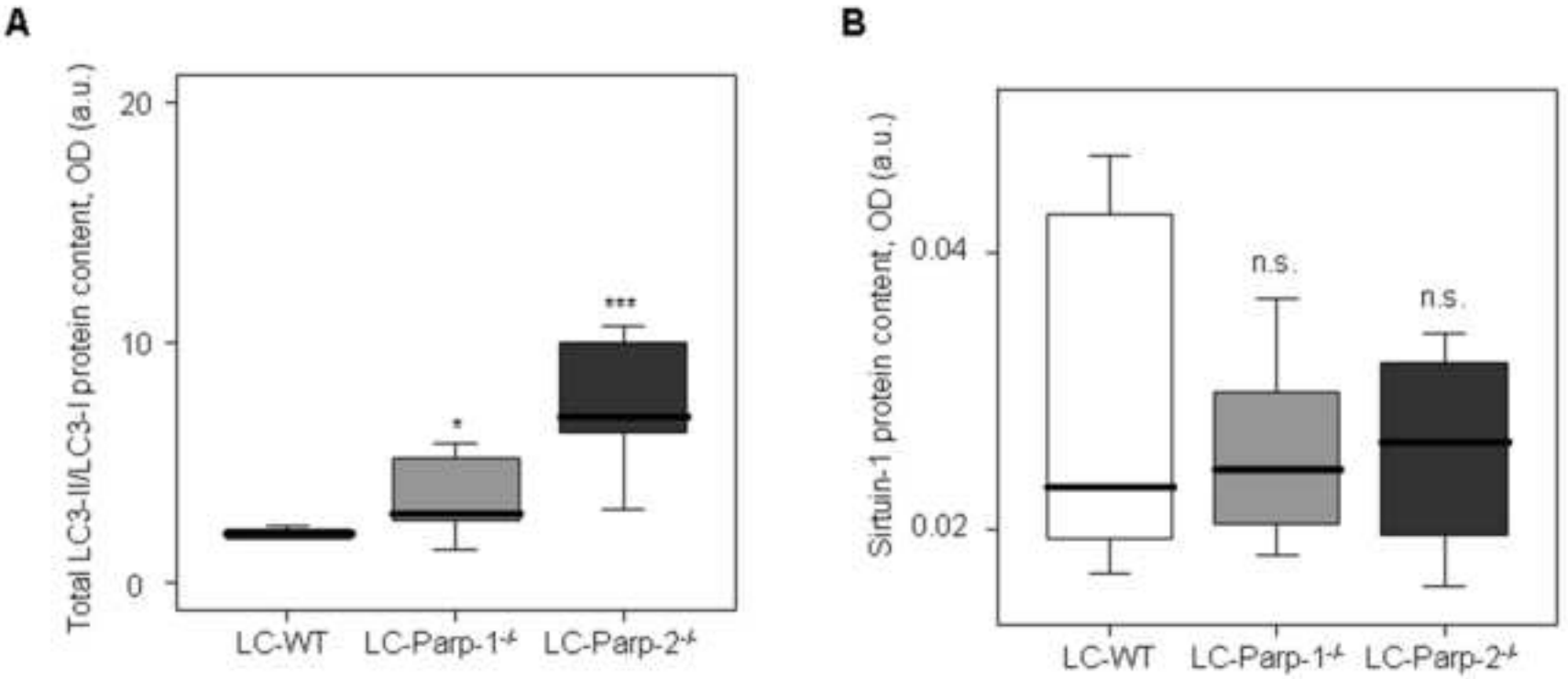

Figure

Click here to download high resolution image

M. Mateu-Jimenez *et al.* Figure 6

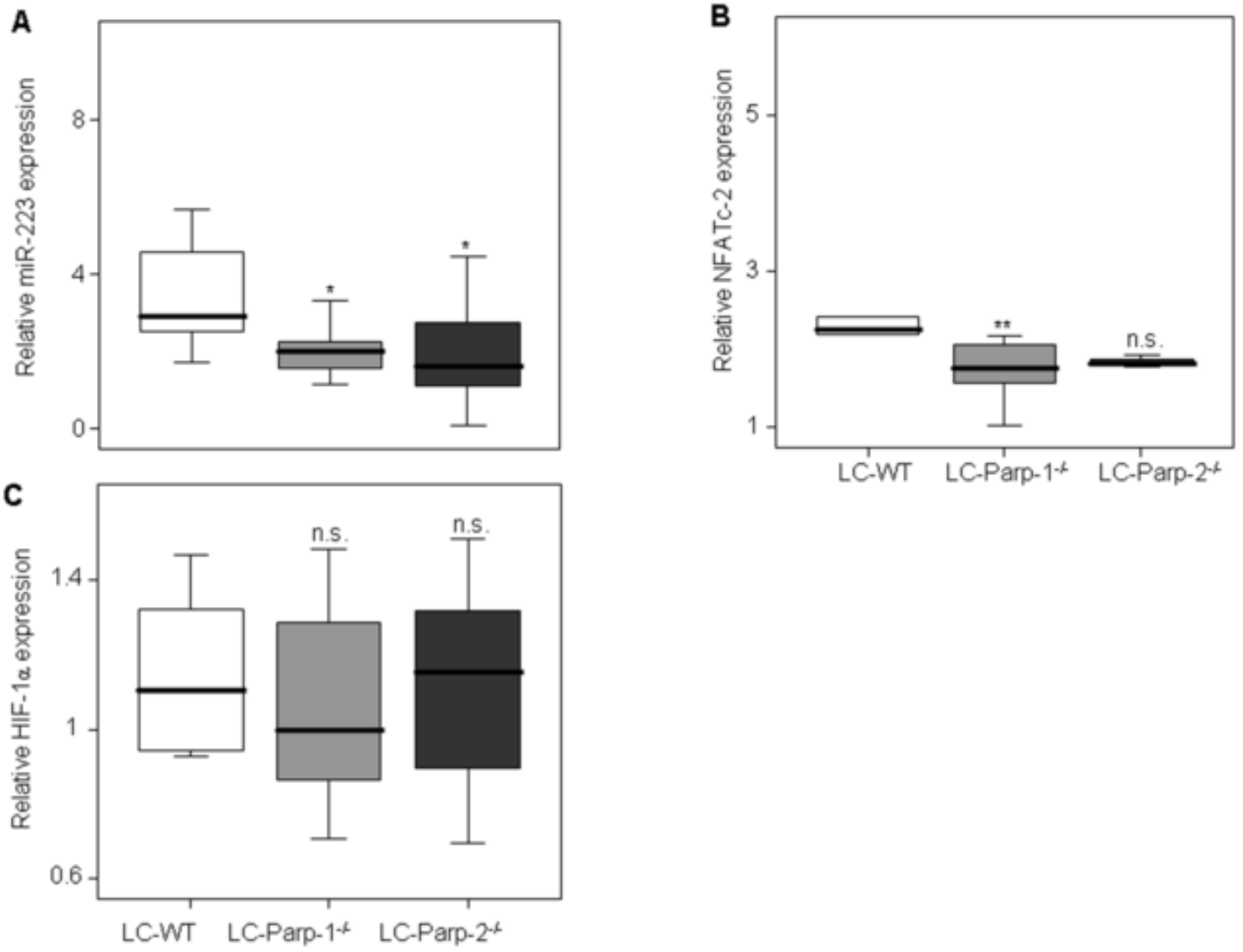

Supplementary Material

Click here to download Supplementary Material: REVISED-PARP-Tumor-Online-Supplement+Figures-20-11-15.docx